Acta Cryst E CRYSTALLOGRAPHIC COMMUNICATIONS

ISSN 2056-9890

Synthesis, crystal structure and properties of *catena*-poly[[[bis(3-methylpyridine-κN)nickel(II)]-di-μ-1,3-thiocyanato] acetonitrile monosolvate]

Christian Näther,* Inke Jess and Christoph Krebs

Institut für Anorganische Chemie, Universität Kiel, Max-Eyth.-Str. 2, 24118 Kiel, Germany. *Correspondence e-mail: cnaether@ac.uni-kiel.de

Received 7 September 2022
Accepted 29 September 2022

Edited by J. Reibenspies, Texas A & M University, USA

Keywords: crystal structure; solvate; nickel thiocyanate; solvent removal.

CCDC reference: 2210399

Supporting information: this article has supporting information at journals.iucr.org/e

In the crystal structure of the title compound, $\{[Ni(NCS)_2(C_6H_7N)_2]\cdot CH_3CN\}_n$, the Ni^{II} cation is octahedrally coordinated by two N-bonding and two S-bonding thiocyanate anions, as well as two 3-methylpyridine coligands, with the thiocyanate S atoms and the 3-methylpyridine N atoms in *cis*-positions. The metal cations are linked by pairs of thiocyanate anions into chains that, because of the *cis*–*cis*–*trans* coordination, are corrugated. These chains are arranged in such a way that channels are formed in which disordered acetonitrile solvate molecules are located. This overall structural motif is very similar to that observed in $Ni(NCS)_2$[4-(boc-amino)pyridine]$_2\cdot CH_3CN$ reported in the literature. At room temperature, the title compound loses its solvent molecules within a few hours, leading to a crystalline phase that is structurally related to that of the pristine material. If the ansolvate is stored in an acetonitrile atmosphere, the solvate is formed again. Single-crystal X-ray analysis at room-temperature proves that the crystals decompose immediately, presumably because of the loss of solvent molecules, and from the reciprocal space plots it is obvious that this reaction, in contrast to that in $Ni(NCS)_2$[4-(boc-amino)pyridine]$_2\cdot CH_3CN$, does not proceed *via* a topotactic reaction.

1. Chemical context

Over the past several years, we and others have been interested in the synthesis and crystal structures of coordination polymers based on transition-metal cations and thiocyanate anions. For this anionic ligand, two major coordination modes are known, which include terminal coordination and the μ-1,3-bridging mode. The latter mode is of special interest if magnetic coordination polymers are to be prepared, because thiocyanate anions can mediate reasonable magnetic exchange (Palion-Gazda *et al.*, 2015; Mekuimemba *et al.*, 2018; Böhme & Plass, 2019; Rams *et al.*, 2020). In the majority of such compounds, the metal cations are octahedrally coordinated by each of two *trans* thiocyanate S and N atoms as well as two N atoms of neutral coligands that mostly consist of pyridine derivatives. The metal cations are linked by pairs of anionic ligands into chains that, because of the all-*trans* coordination, are linear (Shurdha *et al.*, 2013; Prananto *et al.*, 2017; Mautner, Traber *et al.*, 2018; Jochim *et al.*, 2020*a*,*b*).

For octahedrally coordinated metal cations, however, five different isomers exist, which include the all-*trans*, all-*cis* and three *cis*–*cis*–*trans* coordinations. For compounds based on thiocyanate anions, the all-*trans* coordination is the most common, the all-*cis* coordination is unknown and the *cis*–*cis*–*trans*-coordination is very rare. It is noted that the latter coordination leads to the formation of linear chains if the

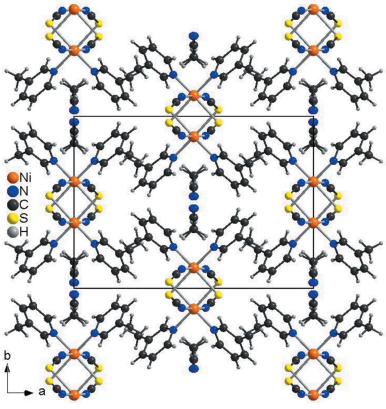

coligands are in the *trans*-position (Werner *et al.*, 2014, 2015*a*,*b*), whereas corrugated chains are observed if they are in the *cis*-position (Böhme *et al.*, 2020; Suckert *et al.*, 2017).

In this context, we have reported on a compound with the composition $Ni(NCS)_2[4\text{-(boc-amino)pyridine}]_2{\cdot}CH_3CN$ in which the Ni^{II} cations are octahedrally coordinated by four μ-1,3-bridging thiocyanate anions as well as two 4-(boc-amino)pyridine ligands (Suckert *et al.*, 2017). The coligands and the S-bonding thiocyanate anions are in *cis*-positions, whereas the two N-bonding anionic ligands are *trans*, leading to the formation of corrugated chains (Fig. 1: top). These chains are interconnected by strong N—H···O hydrogen bonding into layers that are packed in such a way that channels are formed in which disordered acetonitrile solvate molecules are located (Fig. 1: bottom). The acetonitrile molecules can be removed under vacuum and reincorporated *via* the gas phase without any loss in crystallinity. More importantly, single-crystal structure analysis of one crystal showed that the solvent removal is accompanied by a change in symmetry from primitive to *C*-centered. If this crystal is stored in an acetonitrile atmosphere, the solvent is reincorporated and the reflections violating the *C*-centering are observed again. Images of reciprocal space at different acetonitrile contents look like that of a single crystal, but the mosaic spread increases during formation of the ansolvate and reformation of the solvate, which proves that these reactions proceed *via* a topotactic reaction (Suckert *et al.*, 2017).

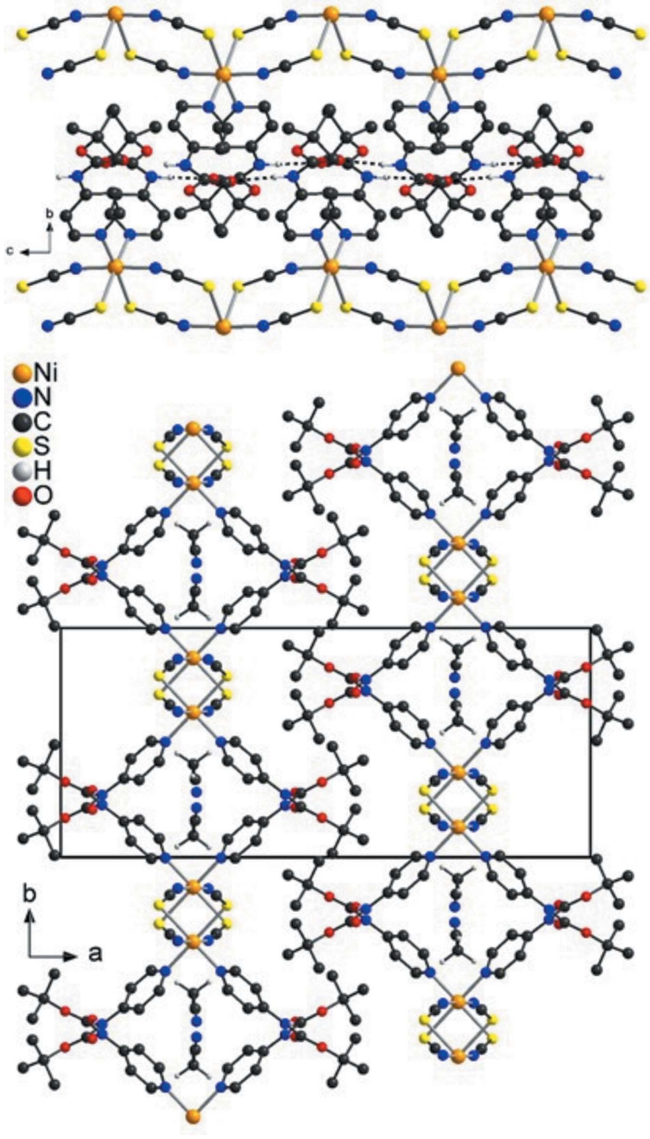

Figure 1
Crystal structure of dithiocyanatobis[4-(boc-amino)pyridine]nickel(II) acetonitrile solvate retrieved from the literature showing a view of the chains with intermolecular N—H···O hydrogen bonding indicated by dashed lines (top) and with a view along the crystallographic *c*-axis (bottom).

In the course of our systematic work we became interested in $Ni(NCS)_2$ compounds based on 3-methylpyridine (3-picoline) as coligand. Many compounds have been reported with this ligand, but with nickel only discrete complexes with a terminal coordination are known and most of these compounds consist of solvates (see *Database survey*). An $Ni(NCS)_2$ compound with 3-methylpyridine that shows a bridging coordination of the anionic ligands does not exist.

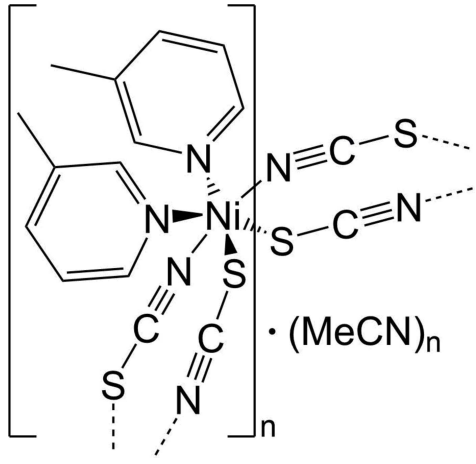

However, in the course of our systematic investigations we accidentally obtained crystals of a further crystalline phase with the composition $Ni(NCS)_2(3\text{-methylpyridine})_2{\cdot}$aceto-acetonitrile. Single-crystal structure analysis shows that a network has formed, which is very similar to that observed in $Ni(NCS)_2[4\text{-(boc-amino)pyridine}]_2{\cdot}$acetonitrile mentioned above. That both compounds are structurally related is already obvious from their similar unit-cell parameters, but also from the crystal symmetry (see *Structural commentary*). X-ray powder diffraction proves the formation of a pure crystalline phase (Fig. S1 in the supporting information). In the IR spectrum, the CN-stretching vibration of the thiocyanate anion is observed at 2109 cm^{-1}, in agreement with the presence of μ-1,3-bridging thiocyanate anions and that of the acetonitrile solvate molecules at 2164 cm^{-1}, proving the presence of acetonitrile (Fig. S2). In view of these results, we investigated whether the acetonitrile solvate molecules can be removed from the title compound and if this proceeds *via* a topotactic reaction as observed in $Ni(NCS)_2[4\text{-(boc-amino)-pyridine}]_2{\cdot}CH_3CN$ mentioned above (Suckert *et al.*, 2017).

Experiments using X-ray powder diffraction show that the crystals have already decomposed at room temperature because of the loss of the solvate molecules, leading to the formation of a crystalline phase. The IR spectrum is very similar to that of the pristine phase but the CN-stretching vibration of the acetonitrile ligands have disappeared, proving that the ansolvate has formed (Fig. S3). The X-ray powder pattern of the ansolvate obtained by storing the title compound for 24 h at room temperature is very similar to that of the pristine material, which indicates that both structures must be strongly related (Fig. S4). In particular, the first three intense reflections are shifted to higher Bragg angles, which is in agreement with a decrease of the unit-cell volume. If the ansolvate is stored for 3 d in a desiccator in an acetonitrile atmosphere, the powder pattern is identical to that calculated for the title compound, which proves that this process is reversible. We also tried to determine the crystal structure of the title compound at room temperature, but during the measurement the crystal started to decompose and no reasonable data were obtained. However, the lattice parameters were determined from indexing the reflections and used for the calculation of the powder patterns. Moreover, from the reciprocal space plots of this data set, it is obvious that the mosaic spread strongly increases, which would be in agreement with a topotactic reaction, but the diffraction pattern does not look like that of a single crystal, as was the case for $Ni(NCS)_2$[4-(boc-amino)pyridine]$_2$·CH_3CN mentioned above (Suckert *et al.*, 2017).

2. Structural commentary

The asymmetric unit of the title compound consists of one Ni^{II} cation, two thiocyanate anions, two 3-methylpyridine ligands and one acetonitrile molecule, all of them located in general positions (Fig. 2). The Ni cations are octahedrally coordinated by two 3-methylpyridine coligands and two N- as well two S-bonding thiocyanate anions in a *cis–cis–trans* coordination with the thiocyanate S atoms and the 3-methylpyridine N atoms in *cis*-positions. The Ni—N and Ni—S bond lengths correspond to those in similar compounds (Table 1). From the bonding angles, it is obvious that the octahedra are slightly distorted (Table 1). This is also obvious from the values of the octahedral angle variance and the mean octahedral quadratic elongation calculated by the method of Robinson *et al.* (1971), which amount to 12.7996 and 1.0190.

The metal cations are linked by pairs of anionic ligands into chains that are corrugated because of the *cis*-coordination of the 3-methylpyridine ligands (Fig. 3).

Table 1
Selected geometric parameters (Å, °).

Ni1—N1	2.0285 (11)	Ni1—S1^{ii}	2.5508 (4)
Ni1—N1^{i}	2.0286 (11)	Ni1—N11	2.0836 (11)
N1—Ni1—N1^{i}	175.54 (6)	S1^{iii}—Ni1—S1^{ii}	87.022 (18)
N1—Ni1—S1^{ii}	83.43 (3)	N11—Ni1—S1^{iii}	173.74 (3)
N1—Ni1—S1^{iii}	93.32 (3)	N11—Ni1—S1^{ii}	89.87 (3)
N1—Ni1—N11	91.71 (4)	N11—Ni1—N11^{i}	93.73 (6)
N1—Ni1—N11^{i}	91.34 (4)		

Symmetry codes: (i) $-x+1, y, -z+\frac{1}{2}$; (ii) $x, -y, z+\frac{1}{2}$; (iii) $-x+1, -y, -z$.

3. Supramolecular features

In the crystal structure of the title compound, the chains proceed in the direction of the crystallographic *c*-axis and are arranged in such a way that cavities are formed, in which disordered acetonitrile molecules are embedded (Figs. 4 and 5). This arrangement is very similar to that observed in $Ni(NCS)_2$[4-(boc-amino)pyridine]$_2$·CH_3CN already reported in the literature (please compare Fig. 1 with Figs. 4 and 5, Suckert *et al.*, 2017). That this structure is structurally related to that of the title compound is also indicated by comparing their unit-cell parameters and their space groups. $Ni(NCS)_2$[4-(boc-amino)pyridine]$_2$·CH_3CN crystallizes in space group

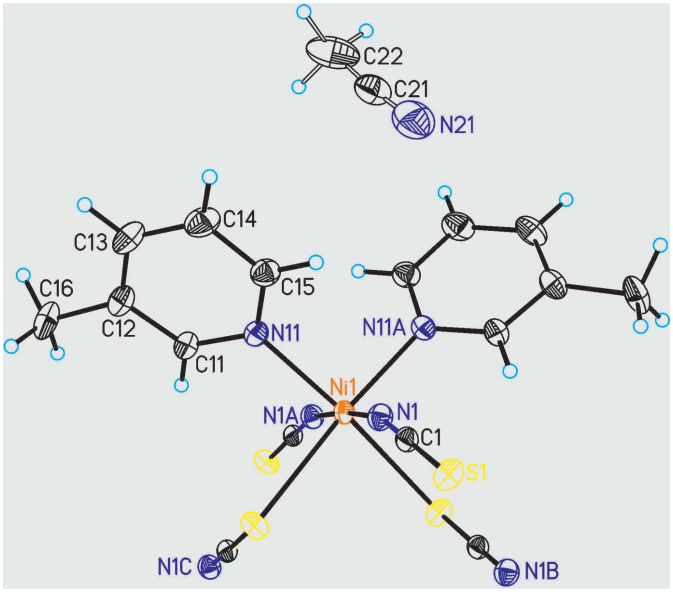

Figure 2
Crystal structure of the title compound with labeling and displacement parameters drawn at the 50% probability level. Symmetry codes: (A) $-x+1, y, -z+\frac{1}{2}$; (B) $-x+1, -y, -z$; (C) $x, -y, z+\frac{1}{2}$.

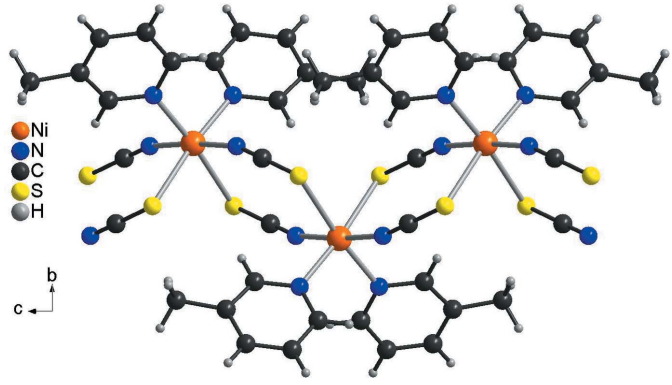

Figure 3
Crystal structure of the title compound with view of part of a chain showing the Ni coordination along the crystallographic *a*-axis.

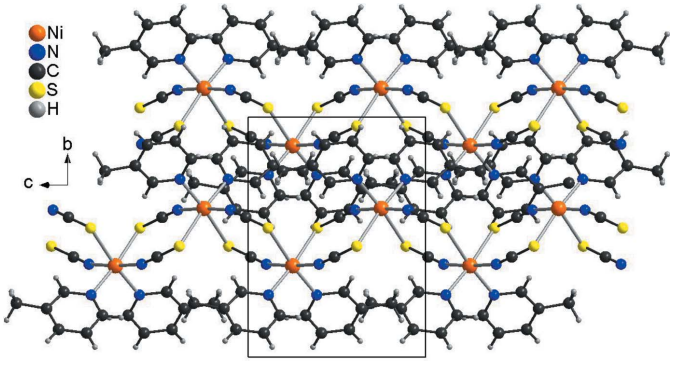

Figure 4
Crystal structure of the title compound with view along the crystallographic *a*-axis.

$P2_1/n$ with a = 26.5715 (7) Å, b = 11.4534 (4) Å, c = 9.8286 (2) Å and β = 94.982 (2)°, whereas the corresponding ansolvate crystallizes in space group $C2/c$ with a = 26.7251 (8) Å, b = 11.3245 (5) Å, c = 9.8036 (3) Å and β = 94.922 (2)°. For a better comparison of the crystal structure of the title compound with that of $Ni(NCS)_2$[4-(boc-amino)-pyridine]$_2$·CH_3CN already reported in the literature, the unit-cell parameters of the title compound must be given for the unconventional setting $I2/c$, leading to values of a = 16.3513 (1) Å, b = 11.7493 (1) Å, c = 9.7383 (1) Å and β = 94.9271 (1)°. The much larger value of the a-axis in the 4-(boc-amino)pyridine compound originates from the much larger size of this neutral coligand, separating the $Ni(NCS)_2$ chains more effectively.

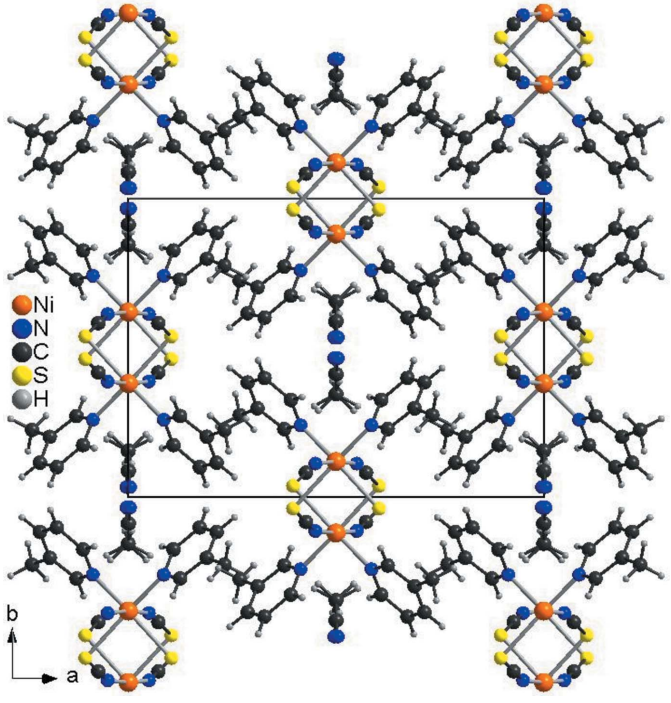

Figure 5
Crystal structure of the title compound with view along the crystallographic *c*-axis.

Finally, it is noted that there are no pronounced intermolecular hydrogen bonds in the title compound, except for one C—H···N contact that is much too long for any significant interaction [C22—H22*A*···N21($1-x$, y, $\frac{1}{2}-z$), H···N = 1.61 Å, C···N = 2.57 (2) Å, C—H···N = 162°]. This is in contrast to $Ni(NCS)_2$[4-(boc-amino)pyridine]$_2$·CH_3CN where the chains are linked by strong N—H···O hydrogen bonding, which might be the reason why this compound is much more stable than the title compound.

4. Database survey

A search in the Cambridge Structure Database (CSD, version 5.43, last update November 2021; Groom *et al.*, 2016) for transition-metal thiocyanate compounds with 3-methylpyridine as coligand leads to several hits. There are a couple of known compounds containing nickel, all of which are discrete complexes of the composition $Ni(NCS)_2$(3-methylpyridine)$_4$ that contain additional solvate molecules such as one molecule per complex of a mixture of dibromo and dichloromethane, of 2,2-dichloropropane and of dichloromethane, as well as two molecules of dichloromethane and trichloromethane (LAYLAY, LAYLEC, LAYLUS, LAYLIG and LAYLOM; Pang *et al.*, 1992). Moreover, crystal structures of the monotrichloromethane (CIVJEW and CIFJEW01; Nassimbeni *et al.*, 1984, 1986) and monotetrachloromethane solvate (JICMIR; Pang *et al.*, 1990) have also been reported. In $Ni(NCS)_2$(3-methylpyridine)$_2$(H_2O)$_2$, two of the coligands are substituted by aqua ligands and no solvate molecules are present (MEGCEH; Tan *et al.*, 2006).

In the discrete copper complex $Cu(NCS)_2$(3-methylpyridine)$_2$ (ABOTET; Handy *et al.*, 2017) the metal center is fourfold and in $Cu(NCS)_2$(3-methylpyridine)$_3$ (VEPBAT; Kabešová & Kožíšková, 1989) fivefold coordinated. Also one more copper compound with the composition Cu(NCS)(3-methylpyridine)$_2$ (CUHBEM; Healy *et al.*, 1984) has been reported in which the cations are tetrahedrally coordinated by two coligands and also two thiocyanate anions, linking them into chains. Some compounds with $Co(NCS)_2$ and 3-methylpyridine can also be found in the CSD. All are discrete complexes, but $Co(NCS)_2$(3-methylpyridine)$_2$ (EYARIG; Boeckmann *et al.*, 2011) has a tetrahedral coordination around the metal center compared to the octahedral complexes $Co(NCS)_2$(3-methylpyridine)$_4$ (EYAROM and EYAROM01; Boeckmann *et al.*, 2011 and Małecki *et al.*, 2012) and $Co(NCS)_2$(3-methylpyridine)$_2$(H_2O)$_2$ (EYAREC; Boeckmann *et al.*, 2011).

With zinc and cadmium, just one compound could be found each, *viz*. the discrete tedrahedral complex $Zn(NCS)_2$(3-methylpyridine)$_2$ (ETUSAO; Boeckmann & Näther, 2011) and $Cd(NCS)_2$(3-methylpyridine)$_2$ (FIYGUP; Taniguchi *et al.*, 1987) with octahedrally coordinated cations that are linked into chains by the thiocyanate anions. Although not yet included in this CSD version, an octahedral iron complex is known, with the cations coordinated by two thiocyanate anions and four 3-methylpyridine ligands (Ceglarska *et al.*, 2022), which was reported analogously also as an isotypic

complex with manganese in the same publication. Otherwise, only one more manganese compound is reported, which however contains 3-methylpyridine-*N*-oxide coligands and consists of a chain structure (KESSAF; Mautner, Berger *et al.*, 2018). There are also two compounds with a mixed-metal composition, on the one hand with *catena*-[tetrakis(thiocyanato)bis(3-methylpyridine)manganesemercury] (NAQYOW; Małecki, 2017*a*) and on the other hand with *catena*-[tetrakis-(μ-thiocyanato)bis(3-methylpyridine)mercuryzinc] (QAMSIJ; Małecki, 2017*b*).

5. Synthesis and crystallization

Synthesis

$Ni(NCS)_2$ was purchased from Santa Cruz Biotechnology and 3-methylpyridine was purchased from Alfa Aesar. Acetonitrile, which was used as the solvent, was dried over CaH_2 before use.

$Ni(NCS)_2$(3-methylpyridine)$_2$·acetonitrile: The reaction mixture containing 0.25 mmol of $Ni(NCS)_2$ (43.7 mg) and 0.25 mmol of 3-methylpyridine (24.3 µl) in 1.5 mL of acetonitrile was stored for 2 days at room temperature, resulting in light-green crystals suitable for single-crystal X-ray diffraction measurements.

Experimental details

The data collection for single-crystal structure analysis was performed using an XtaLAB Synergy, Dualflex, HyPix diffractometer from Rigaku with Cu $K\alpha$ radiation. The PXRD measurements were performed with a Stoe Transmission Powder Diffraction System (STADI P) that is equipped with a MYTHEN 1K detector and a Johansson-type Ge(111) monochromator using Cu $K\alpha_1$ radiation (λ = 1.540598 Å). The IR spectra were measured using an ATI Mattson Genesis Series FTIR Spectrometer, control software: *WINFIRST*, from ATI Mattson. The instruments were calibrated using standard reference materials.

6. Refinement

Crystal data, data collection and structure refinement details are summarized in Table 2. All non-hydrogen atoms were refined anisotropically. The C-bound H atoms were positioned with idealized geometry (methyl H atoms allowed to rotate but not to tip) and were refined isotropically with U_{iso}(H) = 1.2U_{eq}(C) (1.5 for methyl H atoms) using a riding model. The acetonitrile solvate molecules are disordered within the channels around a center of inversion, which is located in the middle of two acetonitrile N atoms that show an N—N distance of 1.151 Å. Therefore, they were refined with an sof of 0.5, leading to reasonable anisotropic displacement parameters. The situation is similar to that in $Ni(NCS)_2$[4-(bocamino)pyridine]$_2$·acetonitrile mentioned above.

It is noted that some additional reflections are observed, leading to a doubling of the unit cell and change from *C*-centered to primitive. The relation between the sub-cell and the super cell is obvious if the super cell [a = 16.3542 (5) Å, b = 23.4916 (8) Å, c = 9.7358 (3) Å and β = 94.977 (3)°, space group $P2_1/c$] is compared with the sub-cell in space group $I2/a$ instead of $C2/c$ [a = 9.7383 (1) Å, b = 11.7493 (1) Å, c = 16.3513 (1) Å and β = 94.927 (1)°]. However, only very few reflections were observed and their intensity is close to zero (Fig. S5). Nevertheless, the structure can easily be refined in space group $P2_1/c$, leading to two crystallographically independent Ni^{II} cations and two unique acetonitrile ligands, but a closer look reveals that even in the super cell the solvate molecules are disordered. Therefore, the very few and weak additional reflections were neglected.

Table 2
Experimental details.

Crystal data	
Chemical formula	$[Ni(NCS)_2(C_6H_7N)_2]\cdot C_2H_3N$
M_r	402.17
Crystal system, space group	Monoclinic, *C*2/*c*
Temperature (K)	100
a, b, c (Å)	18.2934 (9), 11.7472 (4), 9.7341 (5)
β (°)	117.043 (6)
V (Å^3)	1863.11 (17)
Z	4
Radiation type	Cu $K\alpha$
μ (mm^{-1})	3.65
Crystal size (mm)	0.15 × 0.15 × 0.03
Data collection	
Diffractometer	XtaLAB Synergy, Dualflex, HyPix
Absorption correction	Multi-scan (*CrysAlis PRO*; Rigaku OD, 2021)
T_{min}, T_{max}	0.705, 1.000
No. of measured, independent and observed [$I > 2\sigma(I)$] reflections	11840, 1966, 1955
R_{int}	0.015
Refinement	
$R[F^2 > 2\sigma(F^2)]$, $wR(F^2)$, S	0.024, 0.066, 1.07
No. of reflections	1966
No. of parameters	125
H-atom treatment	H-atom parameters constrained
$\Delta\rho_{max}$, $\Delta\rho_{min}$ (e Å^{-3})	0.27, −0.37

Computer programs: *CrysAlis PRO* (Rigaku OD, 2021), *SHELXT2014/5* (Sheldrick, 2015*a*), *SHELXL2016/6* (Sheldrick, 2015*b*), *DIAMOND* (Brandenburg & Putz, 1999) and *publCIF* (Westrip, 2010).

Acknowledgements

This work was supported by the State of Schleswig-Holstein.

References

Boeckmann, J. & Näther, C. (2011). *Acta Cryst.* E**67**, m994.
Boeckmann, J., Reimer, B. & Näther, C. (2011). *Z. Naturforsch. Teil B*, **66**, 819–827.
Böhme, M., Jochim, A., Rams, M., Lohmiller, T., Suckert, S., Schnegg, A., Plass, W. & Näther, C. (2020). *Inorg. Chem.* **59**, 5325–5338.
Böhme, M. & Plass, W. (2019). *Chem. Sci.* **10**, 9189–9202.
Brandenburg, K. & Putz, H. (1999). *DIAMOND*. Crystal Impact GbR, Bonn, Germany.
Ceglarska, M., Krebs, C. & Näther, C. (2022). *Acta Cryst.* E**78**, 755–760.
Groom, C. R., Bruno, I. J., Lightfoot, M. P. & Ward, S. C. (2016). *Acta Cryst.* B**72**, 171–179.
Handy, J. V., Ayala, G. & Pike, R. D. (2017). *Inorg. Chim. Acta*, **456**, 64–75.
Healy, P. C., Pakawatchai, C., Papasergio, R. I., Patrick, V. A. & White, A. H. (1984). *Inorg. Chem.* **23**, 3769–3776.

Jochim, A., Lohmiller, T., Rams, M., Böhme, M., Ceglarska, M., Schnegg, A., Plass, W. & Näther, C. (2020*a*). *Inorg. Chem.* **59**, 8971–8982.
Jochim, A., Rams, M., Böhme, M., Ceglarska, M., Plass, W. & Näther, C. (2020*b*). *Dalton Trans.* **49**, 15310–15322.
Kabešová, M. & Kožíšková, Z. (1989). *Collect. Czech. Chem. Commun.* **54**, 1800–1807.
Małecki, J. G. (2017*a*). *CSD Communication* (refcode NAQYOW). CCDC, Cambridge, England.
Małecki, J. G. (2017*b*). *CSD Communication* (refcode QAMSIJ). CCDC, Cambridge, England.
Małecki, J. G., Bałanda, M., Groń, T. & Kruszyński, R. (2012). *Struct. Chem.* **23**, 1219–1232.
Mautner, F. A., Berger, C., Fischer, R. C., Massoud, S. S. & Vicente, R. (2018). *Polyhedron*, **141**, 17–24.
Mautner, F. A., Traber, M., Fischer, R. C., Torvisco, A., Reichmann, K., Speed, S., Vicente, R. & Massoud, S. S. (2018*a*). *Polyhedron*, **154**, 436–442.
Mekuimemba, C. D., Conan, F., Mota, A. J., Palacios, M. A., Colacio, E. & Triki, S. (2018). *Inorg. Chem.* **57**, 2184–2192.
Nassimbeni, L. R., Bond, D. R., Moore, M. & Papanicolaou, S. (1984). *Acta Cryst.* A**40**, C111.
Nassimbeni, L. R., Papanicolaou, S. & Moore, M. H. (1986). *J. Inclusion Phenom.* **4**, 31–42.
Palion-Gazda, J., Machura, B., Lloret, F. & Julve, M. (2015). *Cryst. Growth Des.* **15**, 2380–2388.
Pang, L., Lucken, E. A. C. & Bernardinelli, G. (1990). *J. Am. Chem. Soc.* **112**, 8754–8764.
Pang, L., Lucken, E. A. C. & Bernardinelli, G. (1992). *J. Incl Phenom. Macrocycl. Chem.* **13**, 63–76.
Prananto, Y. P., Urbatsch, A., Moubaraki, B., Murray, K. S., Turner, D. R., Deacon, G. B. & Batten, S. R. (2017). *Aust. J. Chem.* **70**, 516–528.
Rams, M., Jochim, A., Böhme, M., Lohmiller, T., Ceglarska, M., Rams, M. M., Schnegg, A., Plass, W. & Näther, C. (2020). *Chem. Eur. J.* **26**, 2837–2851.
Rigaku OD (2021). *CrysAlis PRO*. Rigaku Oxford Diffraction.
Robinson, K., Gibbs, G. V. & Ribbe, P. H. (1971). *Science*, **172**, 567–570.
Sheldrick, G. M. (2015*a*). *Acta Cryst.* A**71**, 3–8.
Sheldrick, G. M. (2015*b*). *Acta Cryst.* C**71**, 3–8.
Shurdha, E., Moore, C. E., Rheingold, A. L., Lapidus, S. H., Stephens, P. W., Arif, A. M. & Miller, J. S. (2013). *Inorg. Chem.* **52**, 10583–10594.
Suckert, S., Rams, M., Rams, M. M. & Näther, C. (2017). *Inorg. Chem.* **56**, 8007–8017.
Tan, X.-N., Che, Y.-X. & Zheng, J.-M. (2006). *Chin. J. Struct. Chem.* **25**, 358–362.
Taniguchi, M., Sugita, Y. & Ouchi, A. (1987). *Bull. Chem. Soc. Jpn*, **60**, 1321–1326.
Werner, J., Rams, M., Tomkowicz, Z. & Näther, C. (2014). *Dalton Trans.* **43**, 17333–17342.
Werner, J., Runčevski, T., Dinnebier, R. E., Ebbinghaus, S. G., Suckert, S. & Näther, C. (2015*a*). *Eur. J. Inorg. Chem.* pp. 3236–3245.
Werner, J., Tomkowicz, Z., Rams, M., Ebbinghaus, S. G., Neumann, T. & Näther, C. (2015*b*). *Dalton Trans.* **44**, 14149–14158.
Westrip, S. P. (2010). *J. Appl. Cryst.* **43**, 920–925.

supporting information

Acta Cryst. (2022). E**78**, 1097-1102 [https://doi.org/10.1107/S2056989022009598]

Synthesis, crystal structure and properties of *catena*-poly[[[bis(3-methylpyridine-κ*N*)nickel(II)]-di-μ-1,3-thiocyanato] acetonitrile monosolvate]

Christian Näther, Inke Jess and Christoph Krebs

Computing details

Data collection: *CrysAlis PRO* (Rigaku OD, 2021); cell refinement: *CrysAlis PRO* (Rigaku OD, 2021); data reduction: *CrysAlis PRO* (Rigaku OD, 2021); program(s) used to solve structure: *SHELXT2014/5* (Sheldrick, 2015a); program(s) used to refine structure: *SHELXL2016/6* (Sheldrick, 2015b); molecular graphics: *DIAMOND* (Brandenburg & Putz, 1999); software used to prepare material for publication: *publCIF* (Westrip, 2010).

catena-Poly[[[bis(3-methylpyridine-κ*N*)nickel(II)]-di-μ-1,3-thiocyanato] acetonitrile monosolvate]

Crystal data

$[Ni(NCS)_2(C_6H_7N)_2]\cdot C_2H_3N$
M_r = 402.17
Monoclinic, *C*2/*c*
a = 18.2934 (9) Å
b = 11.7472 (4) Å
c = 9.7341 (5) Å
β = 117.043 (6)°
V = 1863.11 (17) Å^3
Z = 4
F(000) = 832
D_x = 1.434 Mg m^{-3}
Cu *Kα* radiation, *λ* = 1.54178 Å
Cell parameters from 9752 reflections
θ = 4.6–77.2°
μ = 3.65 mm^{-1}
T = 100 K
Plate, light green
0.15 × 0.15 × 0.03 mm

Data collection

XtaLAB Synergy, Dualflex, HyPix diffractometer
Radiation source: micro-focus sealed X-ray tube, PhotonJet (Cu) X-ray Source
Mirror monochromator
Detector resolution: 10.0000 pixels mm^{-1}
ω scans
Absorption correction: multi-scan (CrysAlisPro; Rigaku OD, 2021)
T_{min} = 0.705, T_{max} = 1.000
11840 measured reflections
1966 independent reflections
1955 reflections with $I > 2\sigma(I)$
R_{int} = 0.015
θ_{max} = 77.7°, θ_{min} = 4.6°
h = −23→21
k = −13→14
l = −10→12

Refinement

Refinement on F^2
Least-squares matrix: full
$R[F^2 > 2\sigma(F^2)]$ = 0.024
$wR(F^2)$ = 0.066
S = 1.07
1966 reflections
125 parameters
0 restraints
Primary atom site location: dual
Hydrogen site location: inferred from neighbouring sites
H-atom parameters constrained
$w = 1/[\sigma^2(F_o^2) + (0.0356P)^2 + 1.9913P]$ where $P = (F_o^2 + 2F_c^2)/3$
$(\Delta/\sigma)_{max}$ = 0.001
$\Delta\rho_{max}$ = 0.27 e Å^{-3}
$\Delta\rho_{min}$ = −0.37 e Å^{-3}

Special details

Geometry. All esds (except the esd in the dihedral angle between two l.s. planes) are estimated using the full covariance matrix. The cell esds are taken into account individually in the estimation of esds in distances, angles and torsion angles; correlations between esds in cell parameters are only used when they are defined by crystal symmetry. An approximate (isotropic) treatment of cell esds is used for estimating esds involving l.s. planes.

Fractional atomic coordinates and isotropic or equivalent isotropic displacement parameters (Å²)

	x	*y*	*z*	U_{iso}*/U_{eq}	Occ. (<1)
Ni1	0.500000	0.11950 (2)	0.250000	0.01509 (10)	
N1	0.54965 (7)	0.11278 (9)	0.10148 (12)	0.0185 (2)	
C1	0.57231 (7)	0.08251 (10)	0.01406 (14)	0.0165 (2)	
S1	0.60344 (2)	0.03798 (3)	−0.11091 (4)	0.01977 (10)	
N11	0.58540 (6)	0.24076 (9)	0.38595 (12)	0.0181 (2)	
C11	0.62454 (8)	0.22828 (11)	0.53994 (15)	0.0204 (3)	
H11	0.607248	0.168907	0.584775	0.025*	
C12	0.68901 (8)	0.29758 (12)	0.63729 (16)	0.0244 (3)	
C13	0.71270 (9)	0.38429 (13)	0.56974 (18)	0.0297 (3)	
H13	0.756660	0.433386	0.631780	0.036*	
C14	0.67207 (10)	0.39913 (13)	0.41148 (19)	0.0309 (3)	
H14	0.687354	0.458893	0.363972	0.037*	
C15	0.60876 (9)	0.32557 (12)	0.32326 (16)	0.0240 (3)	
H15	0.581066	0.335802	0.214608	0.029*	
C16	0.73170 (9)	0.27472 (15)	0.80794 (17)	0.0336 (3)	
H16A	0.696992	0.226009	0.835783	0.050*	
H16B	0.741856	0.346916	0.864123	0.050*	
H16C	0.784063	0.236346	0.835127	0.050*	
N21	0.4958 (3)	0.5343 (3)	0.0380 (4)	0.0525 (8)	0.5
C21	0.4990 (2)	0.5882 (3)	0.1369 (4)	0.0366 (7)	0.5
C22	0.4981 (19)	0.6557 (4)	0.238 (3)	0.059 (3)	0.5
H22A	0.511446	0.613590	0.333381	0.089*	0.5
H22B	0.443345	0.689575	0.200183	0.089*	0.5
H22C	0.538683	0.716083	0.258413	0.089*	0.5

Atomic displacement parameters (Å²)

	U^{11}	U^{22}	U^{33}	U^{12}	U^{13}	U^{23}
Ni1	0.01446 (16)	0.01706 (17)	0.01370 (16)	0.000	0.00635 (12)	0.000
N1	0.0176 (5)	0.0201 (5)	0.0177 (5)	−0.0016 (4)	0.0080 (4)	−0.0005 (4)
C1	0.0134 (5)	0.0164 (6)	0.0163 (6)	−0.0017 (4)	0.0039 (4)	0.0010 (4)
S1	0.01886 (16)	0.02257 (18)	0.02138 (17)	−0.00378 (11)	0.01220 (13)	−0.00468 (11)
N11	0.0172 (5)	0.0192 (5)	0.0184 (5)	−0.0010 (4)	0.0084 (4)	−0.0021 (4)
C11	0.0190 (6)	0.0237 (6)	0.0189 (6)	−0.0030 (5)	0.0087 (5)	−0.0027 (5)
C12	0.0199 (6)	0.0288 (7)	0.0245 (6)	−0.0049 (5)	0.0101 (5)	−0.0068 (5)
C13	0.0275 (7)	0.0305 (8)	0.0324 (8)	−0.0124 (6)	0.0148 (6)	−0.0105 (6)
C14	0.0358 (8)	0.0268 (7)	0.0348 (8)	−0.0101 (6)	0.0203 (7)	−0.0018 (6)
C15	0.0271 (6)	0.0223 (6)	0.0245 (6)	−0.0022 (5)	0.0135 (5)	−0.0006 (5)
C16	0.0284 (7)	0.0454 (9)	0.0219 (7)	−0.0141 (7)	0.0070 (6)	−0.0098 (6)

N21	0.071 (2)	0.0457 (19)	0.0431 (19)	−0.0022 (17)	0.0280 (17)	0.0091 (14)
C21	0.0440 (19)	0.0299 (16)	0.0381 (18)	0.0031 (14)	0.0206 (15)	0.0091 (15)
C22	0.080 (3)	0.0398 (18)	0.075 (7)	−0.004 (6)	0.050 (4)	0.017 (6)

Geometric parameters (Å, º)

Ni1—N1	2.0285 (11)	C13—H13	0.9500
Ni1—N1^{i}	2.0286 (11)	C13—C14	1.384 (2)
Ni1—S1^{ii}	2.5508 (4)	C14—H14	0.9500
Ni1—S1^{iii}	2.5508 (4)	C14—C15	1.386 (2)
Ni1—N11^{i}	2.0836 (11)	C15—H15	0.9500
Ni1—N11	2.0836 (11)	C16—H16A	0.9800
N1—C1	1.1590 (17)	C16—H16B	0.9800
C1—S1	1.6456 (13)	C16—H16C	0.9800
N11—C11	1.3435 (16)	N21—C21	1.132 (5)
N11—C15	1.3360 (17)	C21—C22	1.270 (19)
C11—H11	0.9500	C22—H22A	0.9800
C11—C12	1.3912 (18)	C22—H22B	0.9800
C12—C13	1.384 (2)	C22—H22C	0.9800
C12—C16	1.504 (2)		
N1—Ni1—N1^{i}	175.54 (6)	C13—C12—C11	117.29 (13)
N1—Ni1—S1^{iii}	83.43 (3)	C13—C12—C16	122.58 (13)
N1^{i}—Ni1—S1^{iii}	93.32 (3)	C12—C13—H13	120.1
N1—Ni1—S1^{ii}	93.32 (3)	C14—C13—C12	119.72 (13)
N1^{i}—Ni1—S1^{ii}	83.43 (3)	C14—C13—H13	120.1
N1—Ni1—N11	91.71 (4)	C13—C14—H14	120.5
N1—Ni1—N11^{i}	91.34 (4)	C13—C14—C15	119.06 (13)
N1^{i}—Ni1—N11	91.34 (4)	C15—C14—H14	120.5
N1^{i}—Ni1—N11^{i}	91.71 (4)	N11—C15—C14	122.18 (13)
S1^{ii}—Ni1—S1^{iii}	87.022 (18)	N11—C15—H15	118.9
N11^{i}—Ni1—S1^{iii}	173.74 (3)	C14—C15—H15	118.9
N11—Ni1—S1^{ii}	173.74 (3)	C12—C16—H16A	109.5
N11^{i}—Ni1—S1^{ii}	89.87 (3)	C12—C16—H16B	109.5
N11—Ni1—S1^{iii}	89.87 (3)	C12—C16—H16C	109.5
N11—Ni1—N11^{i}	93.73 (6)	H16A—C16—H16B	109.5
C1—N1—Ni1	163.89 (10)	H16A—C16—H16C	109.5
N1—C1—S1	179.13 (12)	H16B—C16—H16C	109.5
C1—S1—Ni1^{ii}	101.56 (4)	N21—C21—C22	174.4 (12)
C11—N11—Ni1	119.96 (9)	C21—C22—H22A	109.5
C15—N11—Ni1	121.53 (9)	C21—C22—H22B	109.5
C15—N11—C11	118.17 (11)	C21—C22—H22C	109.5
N11—C11—H11	118.2	H22A—C22—H22B	109.5
N11—C11—C12	123.56 (12)	H22A—C22—H22C	109.5
C12—C11—H11	118.2	H22B—C22—H22C	109.5
C11—C12—C16	120.10 (13)		
Ni1—N11—C11—C12	172.20 (10)	C11—C12—C13—C14	0.4 (2)

Ni1—N11—C15—C14	−172.51 (11)	C12—C13—C14—C15	−0.8 (2)
N11—C11—C12—C13	0.6 (2)	C13—C14—C15—N11	0.2 (2)
N11—C11—C12—C16	−177.52 (13)	C15—N11—C11—C12	−1.20 (19)
C11—N11—C15—C14	0.8 (2)	C16—C12—C13—C14	178.47 (15)

Symmetry codes: (i) −*x*+1, *y*, −*z*+1/2; (ii) −*x*+1, −*y*, −*z*; (iii) *x*, −*y*, *z*+1/2.